ANALYSIS OF THE OPTIMIZED H TYPE GRID SPRING BY A CHARACTERIZATION TEST AND THE FINITE ELEMENT METHOD UNDER THE IN-GRID BOUNDARY CONDITION

KYUNG-HO YOON*, KANG-HEE LEE, HEUNG-SEOK KANG and KEE-NAM SONG
Korea Atomic Energy Research Institute
150 Deokjin-dong, Yuseong-gu, Daejon, 305-353, Korea
*Corresponding author. E-mail : khyoon@kaeri.re.kr

Received August 17, 2005
Accepted for Publication December 21, 2005

Characterization tests (load vs. displacement curve) are conducted for the springs of Zirconium alloy spacer grids for an advanced LWR fuel assembly. Twofold testing is employed: strap-based and assembly-based tests. The assembly-based test satisfies the in situ boundary conditions of the spring within the grid assembly. The aim of the characterization test via the aforementioned two methods is to establish an appropriate assembly-based test method that fulfills the actual boundary conditions. A characterization test under the spacer grid assembly boundary condition is also conducted to investigate the actual behavior of the spring in the core. The stiffness of the characteristic curve is smaller than that of the strap-wised boundary condition. This phenomenon may cause the strap slit condition. A spacer grid consists of horizontal and vertical straps. The strap slit positions are differentiated from each other. They affords examination of the variation of the external load distribution in the grid spring. Localized regions of high stress and their values are analyzed, as they may be affected by the spring shape. Through a comparison of the results of the test and FE analysis, it is concluded that the present assembly-based analysis model and procedure are reasonably well conducted and can be used for spring characterization in the core. Guidelines for improving the mechanical integrity of the spring are also discussed.

KEYWORDS : Spring Characterization Test, Assembly-based Test, Strap-based Test, Core Condition, Slit, In-grid Condition, Linear Elastic Range, Constraints Condition

1. INTRODUCTION

A spacer grid, one of the most important components of a nuclear fuel assembly, is composed of straps, which are crossed to form an egg crate-like structure [1]. It constitutes the skeleton of the fuel assembly together with guide thimbles and top and bottom end pieces. The primary role of the spacer grid is to hold the fuel rods in an appropriate position between the top and bottom end pieces as well as between the adjacent fuel rods. To this end, the grid strap has springs and dimples that intrude into and contact the fuel rod. In other words, the spacer grid springs and dimples exert a normal contact force on the fuel rod, from which a friction force is produced upon contact. The fuel rod can be positioned in a space due to the friction force. However, the shear force should not be greater than that which would cause the fuel rods to bow during fuel rod growth under reactor operation. These are the constraints in the design of the spring force.

The importance of the spacer grid is advocated further since it should be achieved higher thermal performance. Moreover, increasing the flow mixing around the fuel rods enhances the thermal performance of the grid. This can often be accomplished by incorporating so called '*mixing vanes*' into the grid. In short, better mechanical integrity as well as higher performance of the nuclear fuel cannot be realized without considering improvement of the spacer grids.

Mixing vanes are usually formed on the top of the grid straps. They can be implemented into the grids independently without considering the mechanical integrity. Therefore, the scope of the present study is confined to consideration of the spring force of the spacer grid without referring to the thermal performance since mechanical integrity is the

initial concern.

According to Hooke's law, the spring force is defined to be simply the product of the spring stiffness and the displacement. When a fuel rod is inserted into the spacer grid, the spring and the dimple of the grid are displaced to some extent in the direction of compression (normal to the axial direction of a fuel rod), which is termed '*initial interference*'. The displacement (interference), therefore, depends on the intruded depth of the spring (or the dimple). On the contrary, the stiffness of the spring (or the dimple) is very difficult to determine or to predict *a priori*. It depends on the shape and the dimensions of the spring (or the dimple), such as the thickness of the strap, the width, the fillet radius etc. of the spring (or the dimple). Dimples are usually much stiffer than the spring, and hence is displaced very little as the fuel rod is inserted into the spacer grid. In other words, the spring rather than the dimple is generally the focal point when designing the interference and the contacting force between the fuel rod and the spacer grid. The analysis in this paper deals with the spring only.

The spring force decreases as the fuel burnup increases since the elastic modulus is degraded due to the high temperature in the reactor and the irradiation effect [2]. A cladding collapse due to creep also contributes to a decrease of the spring force. These phenomena should be considered when the initial contacting force between the fuel rod and the spacer grid (termed '*initial spring force*' in general) is designed. When a certain initial spring force is determined in a fuel design, the shape and the interference should be determined tentatively and manufactured. Spring testing is then conducted, whereby the characteristics of the spring, i.e. the curve of the displacement vs. the force, are obtained. The spring force obtained from the curve is checked to assess whether it is acceptable in comparison with the design values. This test is called a '*characterization test*'. The obtained test data is used to determine a design curve of the spring, which is used for the design data of the fuel assembly. Therefore, the characterization test is very important when evolving a new fuel assembly.

This paper addresses two topics: first, a simplified method is studied for the characterization test. In reality, the spring should be tested with a spacer grid assembly itself as the test specimen (assembly-based test). However, the available space for loading is very small due to the dimples and the spring of the adjacent straps, and therefore much care is necessary when conducting an assembly-based test. Both test results are compared to check the usability of the assembly-based test. Second, a finite element (FE) analysis is carried out to verify the simulation capability of the spring tests. By the FE analysis, the half regions of the strap height, i.e. a slit, are identified and modeled. These edges of the horizontal and vertical straps must be modeled for the actual boundary condition. The FE analysis also yields more detailed data of the spring characteristics, and thus this approach is useful for investigating the behavior of a grid spring in the core conditions.

2. CHARACTERIZATION TEST

2.1 Spring Specimen

The springs for the characterization test are made of Zircaloy-4. An optimized H type grid spring, shown in Fig. 1, is tested. Spring (a) is in the outer strap and spring (b) is in the inner strap. Hence, the length of spring B must be shorter than A so as to accommodate the dimples. The widths and length of spring B are different from those of spring A. The difference in the width between the springs of the inner and outer straps is regarded as negligible when compared with that of the length. Two types of characterization test are conducted, a strap-based test and an assembly-based test. The specimen for the assembly-based test is a whole spacer grid assembly and that of the strap-based test is the spring with the strap cut from the grid assembly, as shown in Fig. 1 [3].

Fig. 2 presents the outer and inner grid spring for the Opt. H type spacer grid, respectively.

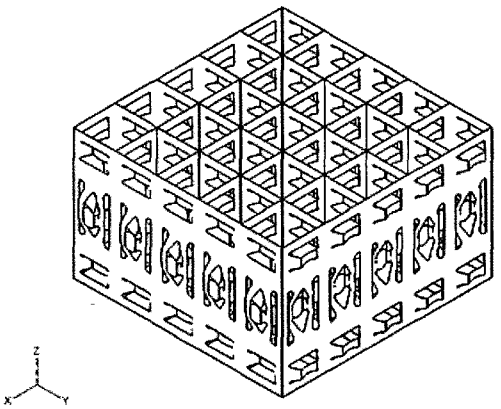

Fig. 1. Schematic Diagram of the 5 × 5 cell Opt. H Type Spacer Grid

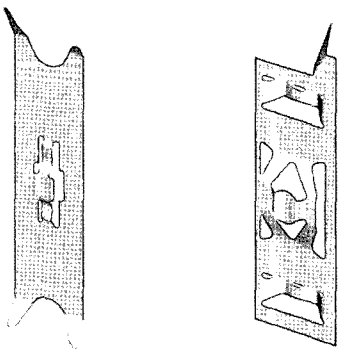

(a) outer (b) inner

Fig. 2. Detailed Drawing of the Unit Outer and Inner Spring for the Opt. H Type Grid

2.2 Apparatus

A universal tensile testing machine (UTM) is used for applying compression onto the spring [4]. A data acquisition system and a personal computer are used for logging the load and the displacement on line. For the strap-based test, the fixture for the specimen and the loading bar are specially designed. The fixture clamps both side edges of the strap specimen, and the loading bar is inserted into the fixture and presses the spring. The fixture and the loading bar for the strap-based test are illustrated in Fig. 3. The loading bar has a cylindrical shape, simulating an actual fuel rod.

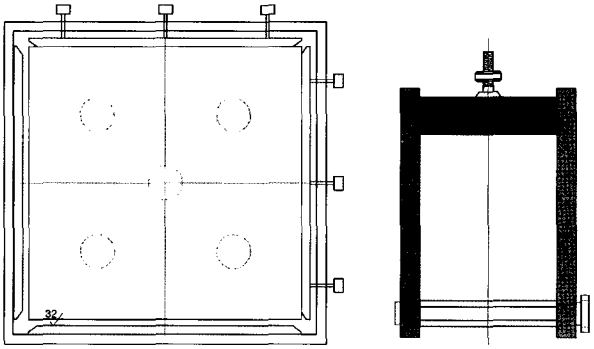

Fig. 3. Schematic Drawings of the Fixture and the Loading Bar

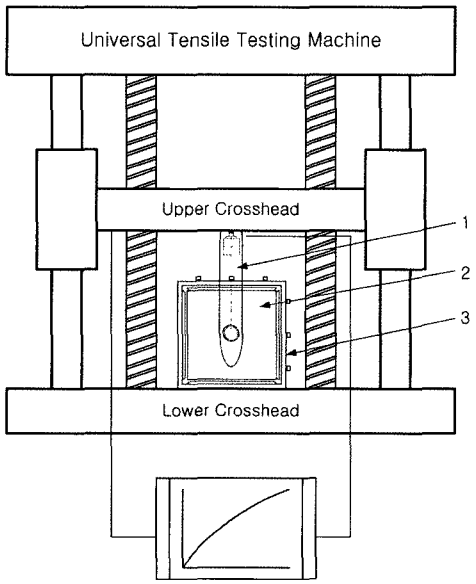

1. Loading Bar
2. Specimen
3. Fixture

Fig. 4. Schematic Diagram for the Assembly-Based Test

For the assembly-based test, a different fixture and loading bar are designed. The fixture clamps four outer surfaces of the grid assembly and is placed on the lower crosshead. The loading bar passes through a specified test location cell of the grid assembly and presses the spring. Four circumferential rod cells are inserted into each fuel rod with a 100mm length. Fig. 4 presents the test setup for the assembly-based test.

2.3 Test Condition

The characterization test (i.e., the assembly-based test) is conducted in a room temperature condition. The cross-head speed is set to be 0.5 mm/min for this test and the sampling rate is five points per second. Five specimens for the assembly-based test are tested repeatedly for one displacement value. Table 1 presents the pre-determined displacements of the Opt. H type grid spring and dimple. Fig. 5 shows the characterization test setup.

Table 1. Displacements for the Characterization Test

Opt. H grid	displacement (mm)
spring	1.2
dimple	0.5

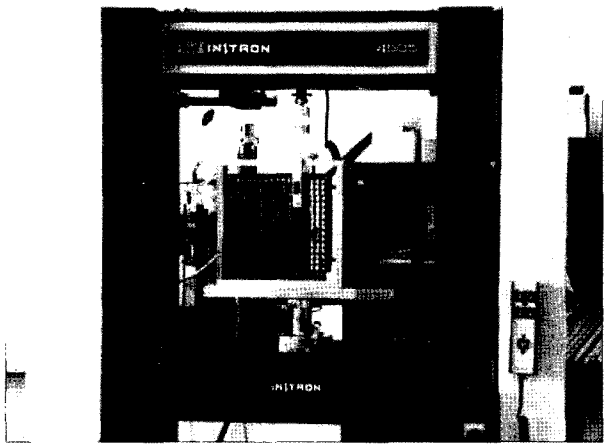

Fig. 5. Test Setup for the Characterization Test

2.4 Characterization Test Results

Typical results of the characterization tests for the spring and dimple, respectively, are given in Figs. 6 and 7. In Figs. 6 and 7, the plots of the assembly-based test are averaged from five specimens at each displacement given in Table 1. For a comparison of the results of the strap-based test

with those of the assembly-based test, the plots are overlapped. Each averaged plot of the strap-based test shows a scattering of the data at several specified displacements with error bars also indicated. The test results show almost the same outcome. The range of the data scattering enables us to conclude that the strap-based test in this study can replace the assembly-based test, thereby providing an easier and time saving method for obtaining the characterization curves.

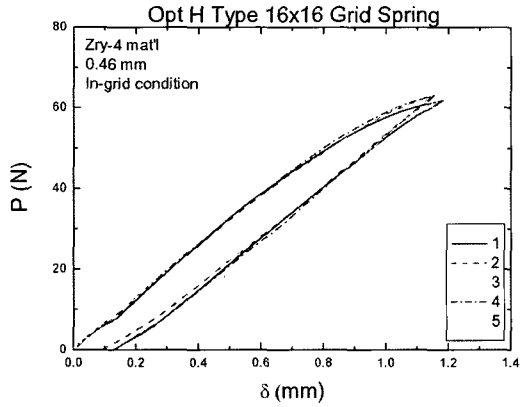

Fig. 6. Characteristic Curve of the Opt. H Type 16 × 16 Grid Spring by the Characterization Test

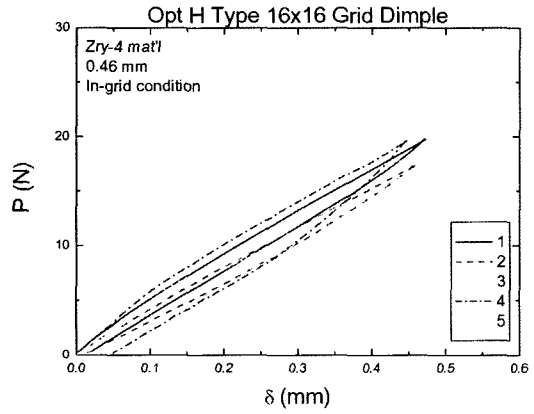

Fig. 7. Characteristic Curve of the Opt. H Type 16 × 16 Grid Dimple by the Characterization Test

For the spring characteristics satisfying the foregoing proposed design requirements, the stiffness of the spring is selected as a performance evaluation parameter. The stiffness is computed by the ratio of the reaction force developed at the final load step and the prescribed displacement. The linear range of the stiffness is also selected as a performance measurement. The stiffness is related to the maximum stress in a model with a nonlinear material property.

Table 2. Test Results of the Opt. H Type Grid Spring and Dimple by the In-Grid Test

No.	Stiffness (N/mm)	
	spring	dimple
1	65.9	39.1
2	64.3	37.7
3	57.4	37.6
4	65.1	38.7
5	67.7	36.4
average	64.1	37.9

Table 2 presents the characteristic curve of the Opt. H type grid spring and dimple. The average stiffness of the Opt. H type grid spring is 64.1 N/mm, and the maximum load is about 62 N. In addition, the plastic set is about 0.11 mm after 1.2 mm loading. These results are very different from those of the strap-based test.

2.5. Test Results Verification

In order to verify the characterization test results, the current results were compared with those of previous test results reported by Westinghouse [5]. This previous test method is different from the current test method. While the latter Westinghouse used a testing finger within a spring cell, as shown in Fig. 8, the the present study employs a universal tensile testing machine.

Therefore, the present test method needs to be verified by a reported value. The characteristic curve of the inner

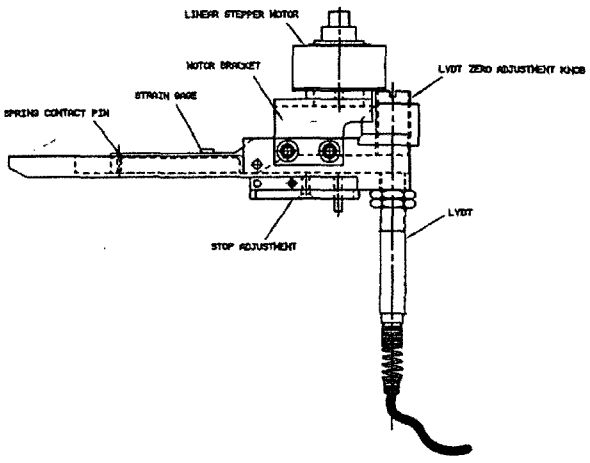

Fig. 8. In-Grid Spring Tester Used by Westinghouse

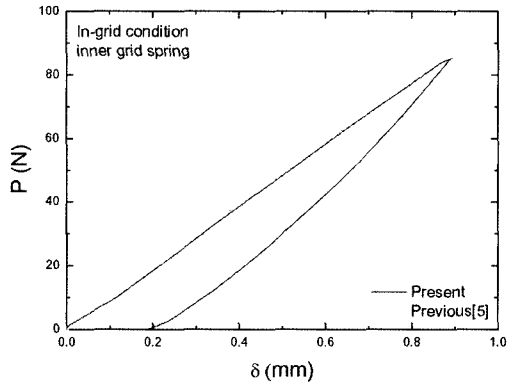

Fig. 9. Characteristic Curves of the Inner Grid Spring From the Two Tests

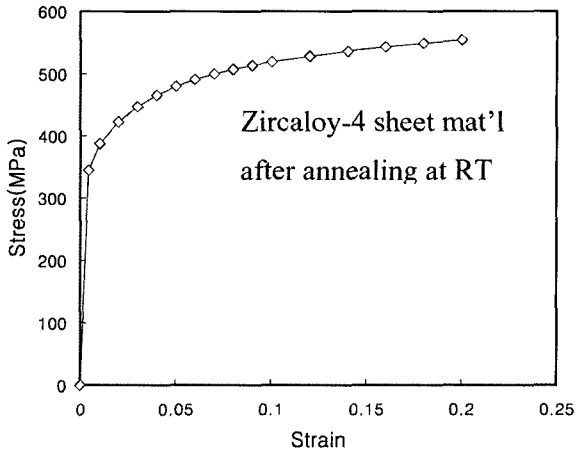

Fig. 10. True Stress Vs. True Strain Curve of Zircaloy-4 Sheet Material From Tensile Test [8]

grid spring according to the above two test results is shown in Figure 9.

The average spring stiffness of the inner grid spring was 98.4 N/mm according to Westinghouse, and value from the present results was 97.9 N/mm. The difference between the two is approximately 0.5 %. The average spring stiffness of the outer grid spring was 156.6 N/mm according to the Westinghouse, and that of the present work was 146.1 N/mm. The difference between the two is roughly 6.7 %. Therefore, the present test method is in good agreement with the previous results.

3. FINITE ELEMENT ANALYSIS

3.1 Geometry and Material Properties

The characterization test of the spring was simulated by the finite element method. The commercial codes I-DEAS [6] and ABAQUS [7] were used for the FE analysis. The geometric data for the FE analysis followed that for the specimen of the spring test.

The material of the plate is Zircaloy-4, its elastic modulus is 108.3 GPa, yield strength is 344.3 MPa, density is 6550 kg/m^3, and Poisson's ratio is 0.34. The characteristic behavior of the grid spring was considered to be plastic deformation phenomena, and therefore the mechanical properties of the material had to be considered in a piece-wise linear elastic-plastic characteristic curve. Therefore, a uni-directional tensile test of the material was accomplished with ASTM [8]. The elastic-plastic material properties of the Zircaloy-4 were summarized and the true stress and strain data was converted from the engineering stress and strain data, as shown in Figure 10 [8].

3.2 FE Model and Boundary Conditions

4-node shell elements were used for the FE model of the springs because the thickness of the strap (0.457 mm) was much smaller than the width (12.85 mm) [9]. A thin shell element was used when the transverse shear flexibility was negligible, and as such the Kirchhoff constraint must be satisfied accurately. In the case of a homogeneous material, the shell element is generally used when the thickness is less than about 1/15 of the characteristic length, which is calculated from the surface data of the shell. The 4-node shell element (S4R) in ABAQUS satisfies the above geometrical dimension and also procures the Kirchhoff constraint.

A 5 ×5 cell array partial grid was prepared for simulating the assembly-based characteristic analysis. The circumferential fuel rod cells were inserted with four rigid fuel rods to simulate the in-grid boundary conditions. Figure 11 presents the final FE model for the FE analysis.

For the boundary conditions of the FE analysis, all *dofs* at the outer edges were constrained since the fixture clamps those edges of the spring specimen during the assembly-based characterization test. The condition also holds true

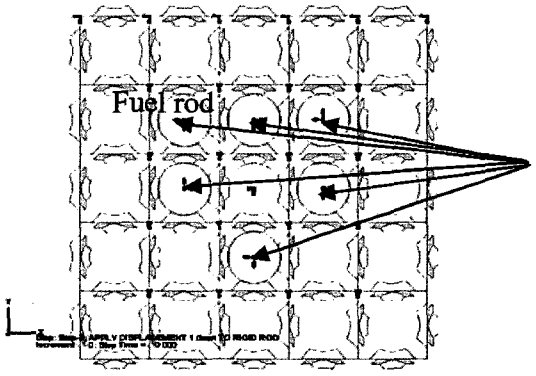

Fig. 11. FE Model of the Opt. H 5 × 5 cell Grid for the Assembly-Based Characteristic Analysis

in the assembly-based test since the edges are constrained by the adjacent perpendicular straps.

In Figure 12, the node set of the horizontal straps (HORIZONTAL) is constrained with an x-translational dof due to the vertical straps. In the same manner, the node set of the vertical straps (VERTICAL) is constrained with a y-translational dof due to the horizontal straps, as shown in Figure 13. The fuel rods and the supports of the strap were defined as a master and a slave surface.

For the HORIZONTAL node set case,

$$U_{X,HORIZON.} = 0$$
$$ROT_{Y,HORIZON.} = 0.$$

For the VERTICAL node set case,

$$U_{Y,VERTI.} = 0$$
$$ROT_{X,VERTI.} = 0.$$

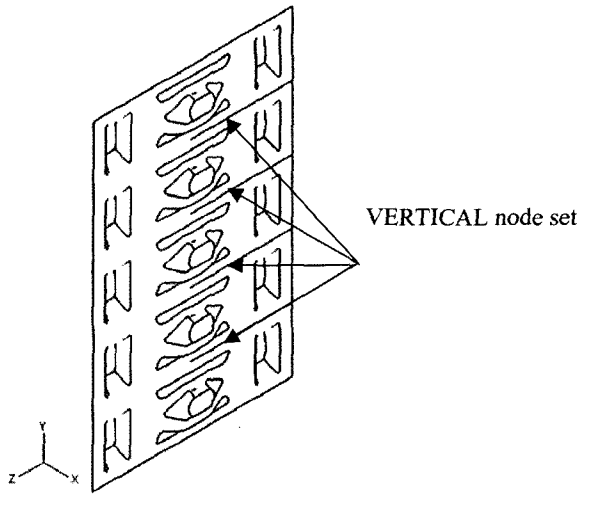

Fig. 13. VERTICAL Node Set for the In-Grid Boundary Condition

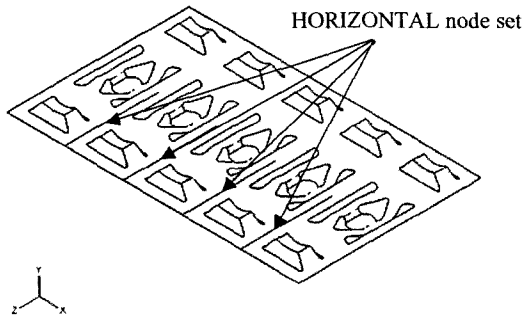

Fig. 12. HORIZONTAL Node Set for the In-Grid Boundary Condition

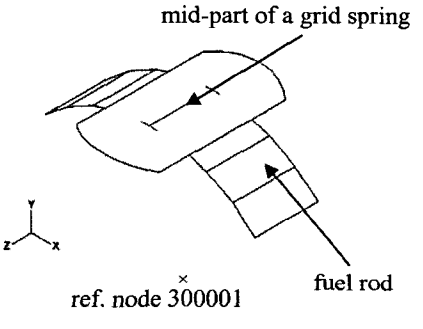

Fig. 14. Configuration of the Contact Surface Between the Grid Spring and the Fuel Rod

The compressive load onto the spring was simulated by displacing a rigid rod, initially contacting the top of the spring, up to a specified distance. These fuel rods were defined as a master surface, because the stiffness of the fuel rod is much higher than that of the supports. Hence, they only have translational motion *dofs*. Figure 14 presents the initial displacement due to the displacement of a fuel rod for the reference node (300001) of the SPRING node set. By the displacement of the rigid rod, the applied load to the spring was obtained from the reaction force at the reference node of a center fuel rod.

3.3 FE Results and Discussion

The characteristic results of the Opt. H type grid spring obtained by the FE analysis are shown in Figure 15. A linear curve for the characteristic behavior is presented until the pre-defined displacement. The stiffness of the grid spring at the minimum linear region was 67.0 N/mm. The in-grid characteristic behavior of the Opt. H type grid spring was obtained only for the loading condition.

Figure 16 presents the von Mises stress configuration at the initial interference step due to the insertion of several fuel rods. In this figure, the maximum von Mises equivalent stress occurs at the support edges of the grid spring due to the fuel rod insertion. All support parts of the strap had stress in spite of the before loading condition. As expected, the value was much lower than the allowable yield strength of Zircaloy-4.

Figure 17 presents the von Mises equivalent stress configuration for the 1.2 mm displacement loading case. At this time, the maximum stress value was 434 MPa, which was much higher than that of the allowable yield strength. Therefore, a plastic deformation region exists due to the excessive loading.

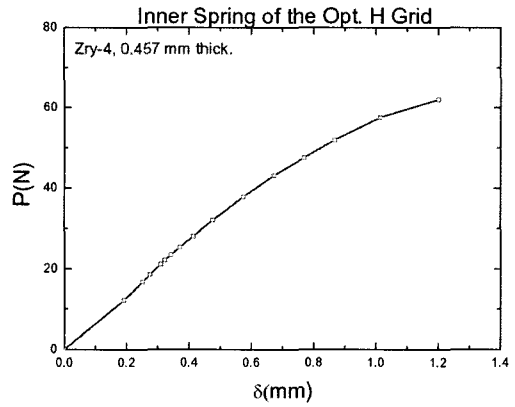

Fig. 15. Characteristic Curve of the Opt. H Type Inner Grid Spring From the Test and the FE Analysis Method

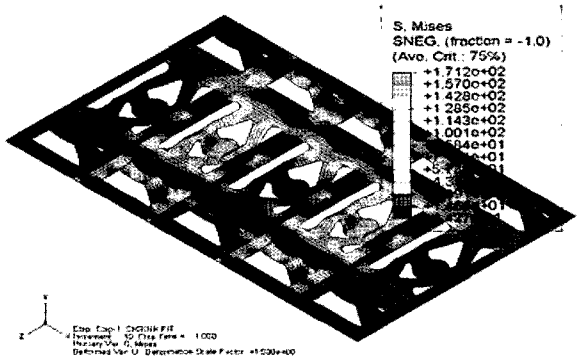

Fig. 16. Von Mises Equivalent Stress Contour at the Initial Interference Step Due to the Fuel Rod Insertion From FE Analysis

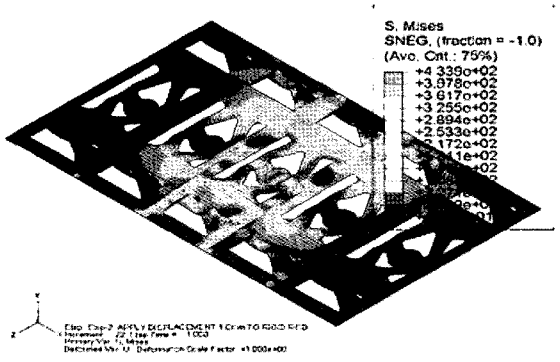

Fig. 17. Von Mises Stress Contour at a 1.2 mm Displacement From the FE Analysis

Figure 18 presents the deformed shape after the 1.2 mm displacement. In this figure, the deflections mainly occurred in the y-direction for all the neighboring cells. In particular, the displacements of the front half edge, i.e. the HORIZONTAL node set, of the horizontal straps took place in the y-direction. This phenomena is quite different from that observed in the strap-based case. This state affects the reduced stiffness in the fuel rod supporting condition. Therefore, the supporting behavior of the grid spring must be considered in the in-grid condition characteristic.

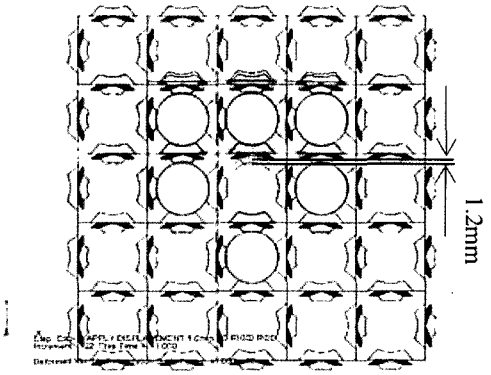

Fig. 18. Deformed Shape at 1.2mm Displacement According to the FE Analysis

4. COMPARISON AND DISCUSSION

4.1 Comparison of the Characteristic Test by the Two Methods

The stiffness of the inner and outer grid spring under the in-grid condition was in good agreement, respectively, with the previous results. Although the previous test method is more easily utilized than the current method, it cannot be applied to every supporting shape due to the specialty of the finger sensor. The test results from the two methods are summarized in Table 3.

Table 3. Comparison of the Grid Spring Stiffness Between the Two Test Methods

Classification	stiffness (N/mm)	
	inner	outer
previous	98.4	156.6
current	97.9	146.1

4.2 Comparison of the Characteristic Curve by Test and FE Analysis Method

The above FE analysis results were compared with those obtained by the test, yielding good agreement with only a slight discrepancy of 1.0 %, as shown in Fig. 19 The characteristic behavior of the in-grid condition has a nearly linear curve until 0.6 mm displacement for both methods. From the above results, the discrepancy after the 0.6 mm displacement appears to be caused by the mechanical properties of the base material, non-linearity due to the large displacement, the applied analysis boundary condition, and non-uniform thickness of the grid spring due to the plastic forming process.

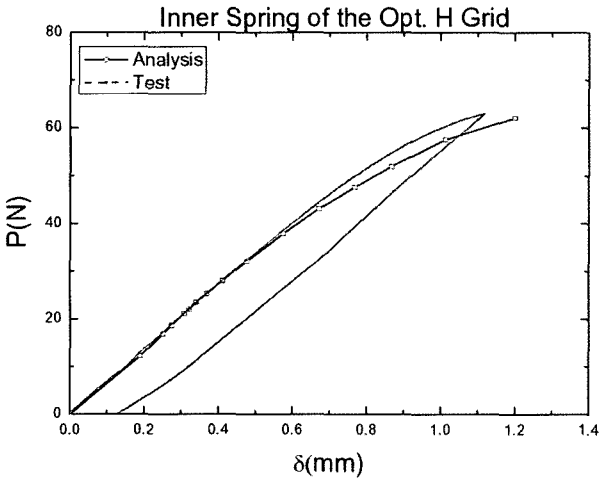

Fig. 19. Comparison Result Between the Characterization Test and FE Analysis

5. CONCLUDING REMARKS

An in-grid test method for characterizing the spacer grid spring is studied with the aim of satisfying the intrinsic boundary condition of the grid assembly. Consequently, the analysis result has been verified through comparison with the reported value. Although the outer grid spring is slightly different from that employed in the previous study, the current method is a suitable test procedure for obtaining the characteristic curve of a grid spring under the in-grid boundary condition.

A finite element analysis could simulate the characterization curves obtained via the test. The stress field in the spring was investigated by the FE analysis, from which we could confirm that the stress values were much higher at the fillets and corners. This phenomenon becomes more severe as the radii of curvature of the spring become smaller, as expected. When the spring is pressed beyond the displacement at the peak load of the characteristic curve, the area of the stress is larger than the yield strength expansion. This causes the spring to change shape, which results in a decrease in stiffness.

The developed FE model and the analysis procedure could be useful tools for predicting the characteristic behavior of a grid spring under an in-grid condition.

ACKNOWLEDGEMENT

This work was financially supported by the nuclear R&D program of the Ministry of Science and Technology of Korea.

REFERENCES

[1] K. N. Song et. al., Fuel Assembly Mechanical Design and Engineering, KAERI, (1986).
[2] K. N. Song and Kunz, Design of the Fuel Assembly Structure with Zircaloy Spacer Grids, KAERI/KWU Work Report, U6 312/87/e278, (1987).
[3] K. H. Yoon et al., Spacer Grid for Nuclear Reactor Fuel Assemblies with Grid Springs Maintaining Conformal Contact with Fuel Rods and Enlarged Elastic Range, US Patent No. 6707872, (2004).
[4] W. G. Kim and D. W. Kim, Tensile Test Procedure of INSTRON 4505, NMTD-RI&DB-TECHMEMO 001/1999, Rev. 00, (1999).
[5] K. T. Kim et. al., Development of Advanced Nuclear Fuel for KSNPs, Final Research Report, KNFC, (2002)
[6] I-DEAS User's Manual, Ver. 10Nx, Structural Dynamics Research Corporation, OH, USA, (2003).
[7] ABAQUS/Standard User's Manual (version 6.4), ABAQUS Inc., Pawtucket, R.I., USA, (2004).
[8] ASTM E8M-99, Standard Test Methods for Tension Testing of Metallic Materials, (1999).
[9] H. K. Kim and K. H. Yoon, Analysis of Fuel Grid Spring by Characterization Test and Finite Element Method, Proceedings of ICONE 8, Paper No. ICONE-8235, (2000).